

GFD 2012 Lecture 4 Part II: Rapidly rotating convection

Jeffrey B. Weiss; notes by Alban Sauret and Vamsi Krishna Chalamalla

June 21, 2012

1 Introduction

Rapidly rotating convection constitutes an interesting mathematical system, and is relevant in geophysics and oceanography, for example, in the phenomenon of ocean deep convection. However, the rapid rotation and strong thermal forcing found in natural systems is inaccessible to numerical simulations of the underlying Boussinesq equation. By applying an asymptotic expansion one obtains reduced equations for non-hydrostatic quasi-geostrophic dynamics that allows one to reach regimes of rapid rotation and strong thermal forcing. Some results of numerical simulations and a model to describe those results will be presented, in particular the regime where coherent convective plumes are obtained.

1.1 Ocean deep convection

Figure 1.a presents the global thermohaline circulation on Earth. Sinking water is present in the Atlantic, in the Antarctic that creates a global overturning which circulates around the globe. It also raises the question of how the water gets to the top or to the bottom of the ocean. Note that the timescale of this motion is roughly 1000 years. The intermittent sinking takes place on very small scales and is relatively fast. Therefore, different time and length scales are present in this problem which makes it difficult to simulate. Figure 1.b shows zones where deep and bottom or intermediate waters form and sink and the major broad scale upwelling zone. This circulation of waters, has a large impact on the global climate and therefore constitutes an important topic.

1.2 Phases of deep convection

The phenomenon of deep convection [1] shows three major phases: a preconditioning phase where a cyclonic gyre of length scales $L \sim 100$ km domes isopycnals making the density more uniform; then, there is a deep convecting phase where cooling events trigger deep plumes of length scales $L \sim 1$ km; finally these plumes organize and creating geostrophic eddies that have scales about $L \sim 10$ km. In the following discussion, plumes of length scales $L \sim 1$ km are considered.

1.3 Rotation and deep convection

Before going further, it is important to notice that the deep convection is influenced by rotation. Indeed, it occurs in polar latitude where the Coriolis parameter f is large. Thus,

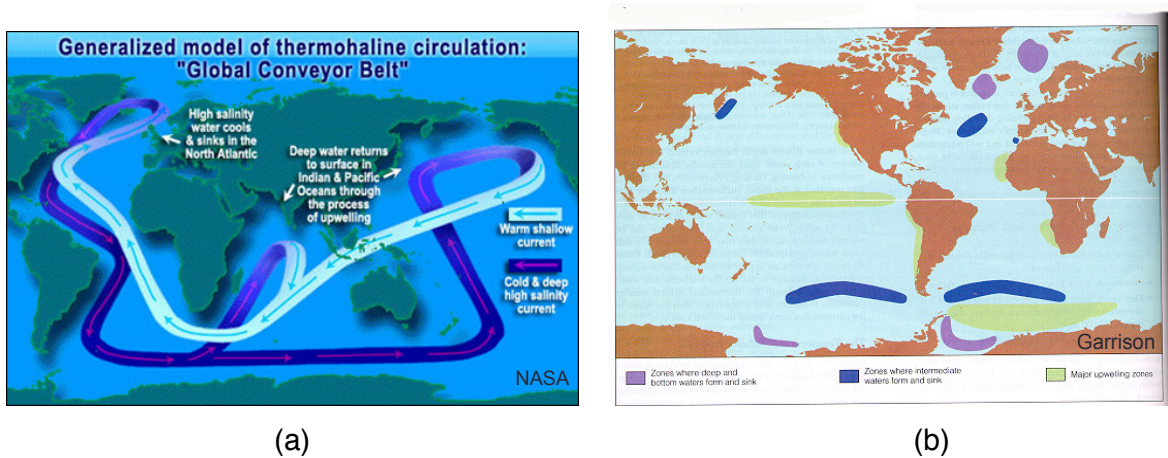


Figure 1: (a) Schematic of a generalized model of thermohaline circulation showing the Global Conveyor Belt. (b) Schematic of the principal zones where deep and bottom (in purple) or intermediate waters (in blue) form and sink and the major upwelling zone (in green).

we can define a natural Rossby number R_0^* such that

$$R_0^* = \frac{L_{rot}}{H} = \sqrt{\frac{B}{f^3 H^2}} \quad (1)$$

where L_{rot} is the horizontal rotational scale, H the height, and B the buoyancy flux. Observations show that $R_0^* \sim 0.1 - 0.4$.

2 Non-hydrostatic quasi-geostrophic model

The traditional quasigeostrophic approximations result from assuming rapid rotation, strong stable stratification, hydrostatic balance (vertical pressure gradients are balanced by gravity), and geostrophy (horizontal pressure gradients are balanced by the Coriolis force). This results in a diagnostic relation for the geostrophic velocity. By going to higher order, one obtains a prognostic equation for the time evolution.

Here, a non-hydrostatic quasi-geostrophic model [2, 3] is considered. We start with Boussinesq equations in a rapidly rotating regime, i.e. the Rossby number is small, $R_0 = \epsilon \ll 1$. Usually structures in ocean and atmosphere have a large horizontal scale and a small vertical scale. But if we now consider structures such as convective plumes, they are tall and thin which imply $A_z = H/L = 1/\epsilon \gg 1$.

Then, a multiscale asymptotic expansion is done, assuming a large vertical scale $Z = z/A_z = \epsilon z$. It also requires a slow time T defined by $T = \epsilon^2 t$. Then, using asymptotic expansions, the partial derivatives in the vertical direction and time become

$$\partial/\partial z \rightarrow \partial/\partial z + \epsilon \partial/\partial Z \quad \text{and} \quad \partial/\partial t \rightarrow \partial/\partial t + \epsilon^2 \partial/\partial T. \quad (2)$$

Considering a Reynolds decomposition where averaging is done over the fast space and fast time results in mean equations for the slow vertical scale and slow time

$$\bar{\mathbf{u}}(Z, T) = \int dx dy dz dt \mathbf{u}(x, y, z, t, Z, T). \quad (3)$$

Define the velocity fluctuation as $\mathbf{u}' = \mathbf{u} - \bar{\mathbf{u}}(Z, T)$. Using asymptotic analysis both the mean velocity and the fluctuation term are expanded in powers of ϵ :

$$\bar{\mathbf{u}} = \bar{\mathbf{u}}_0 + \epsilon \bar{\mathbf{u}}_1 + \dots \quad \text{and} \quad \mathbf{u}' = \mathbf{u}'_0 + \epsilon \mathbf{u}'_1 + \dots \quad (4)$$

The vertical momentum equation gives the leading balances for the first-order terms:

$$\frac{\partial \bar{p}_0}{\partial Z} = \Gamma \bar{\theta}_0 \quad (5)$$

which says that the mean state hydrostatic at lower order, where p is the pressure, θ is the temperature, Γ the non-dimensional buoyancy frequency defined by: $\Gamma = B L/U^2$. The horizontal momentum equation to lowest order is

$$\bar{\mathbf{u}}_0 = \mathbf{0} \quad \text{and} \quad \hat{\mathbf{z}} \times \mathbf{u}'_0 = -\nabla p'_1. \quad (6)$$

Therefore, at lowest order, the mean velocity is zero and the fluctuation of the velocity field is in geostrophic balance.

These lowest order equations lead to some implications. Geostrophy implies horizontal non-divergence, $\nabla_{\perp} \cdot \mathbf{u}'_{0\perp} = 0$ and then the vertical velocity is independent of z , $\partial w'_0 / \partial z = 0$. In a traditional QG model, this leads to $w'_0 = 0$ since layer is thin and $w_0 = 0$ on boundaries. But here, because of the multiple length scales, we just have no fast z derivatives, so $w'_0 \neq 0$ remains possible provided it only depends on slow Z . Thus, the lowest order velocity can have a slow vertical scale dependence: $w'_0 = w'_0(x, y, Z)$. As a results, the first order fluctuations are non-hydrostatic.

To write the equations of motion, we use the usual toroidal and poloidal decomposition through the streamfunctions Ψ and ϕ which are defined by

$$\mathbf{u}' = -\nabla \times \Psi \hat{\mathbf{z}} - \nabla \times \nabla \times \phi \hat{\mathbf{z}}. \quad (7)$$

We therefore can write

$$\mathbf{u}'_0 = \begin{pmatrix} -\partial \Psi_0 / \partial y \\ \partial \Psi_0 / \partial x \\ \nabla_{\perp}^2 \phi_0 \end{pmatrix} \quad (8)$$

where $\phi_0 = \phi_0(x, y, Z)$ and has no fast z variation. The first two terms are given by the function Ψ in the usual way and the last terms, $\nabla_{\perp}^2 \phi_0$ gives a non-hydrostatic vertical velocity that shows the difference with the classical quasi-geostrophic model.

3 Rotating Rayleigh-Bénard convection

3.1 Non-dimensional parameters

The length scale is chosen such that the Reynolds number is unity, $Re = 1$. The remaining parameters describing the problem are the scaled Rayleigh number: $\tilde{Ra} = E^{4/3} Ra$, which defines the strength of the buoyancy frequency, where E is the Ekman number defined by $E = \nu/(2\Omega H^2)$, and the Prandtl number σ which represents the ratio of momentum to heat diffusion. This scaling of E and Ra is based on the critical Rayleigh number for the initial instability in the presence of rotation. In the following sections, numbers indicating order are dropped but the lowest order in all cases are kept.

3.2 Reduced equation

The vertical velocity equation is:

$$\frac{\partial w}{\partial t} + J(\Psi, w) + \frac{\partial \Psi}{\partial Z} = \frac{\tilde{Ra}}{\sigma} \theta' + \nabla_{\perp}^2 w \quad (9)$$

where θ' is the temperature fluctuation, and J is the Jacobian defined by

$$J(A, B) = \frac{\partial A}{\partial x} \frac{\partial B}{\partial y} - \frac{\partial A}{\partial y} \frac{\partial B}{\partial x}. \quad (10)$$

In this equation, $\partial w/\partial t$ is the vertical velocity tendency, $J(\Psi, w)$ represents the horizontal advection of vertical velocity. Note that there is no vertical advection. The term $\partial \Psi/\partial Z$ is the unbalanced vertical pressure gradient which forces vertical velocity, $\tilde{Ra} \theta'/\sigma$ is the buoyancy forcing term and finally $\nabla_{\perp}^2 w$ is the horizontal dissipation.

The equation for the vertical vorticity defined by $\omega = \nabla_{\perp}^2 \Psi$ is:

$$\frac{\partial \omega}{\partial t} + J(\Psi, \omega) - \frac{\partial w}{\partial Z} = \nabla_{\perp}^2 \omega \quad (11)$$

Here, $\partial \omega/\partial t$ is the vertical vorticity tendency, $J(\Psi, \omega)$ the usual horizontal advection of vertical vorticity, $-\partial \omega/\partial Z$ represents a stretching term where vertical velocity gradients on large scales spin up vorticity and implies an ageostrophic horizontal divergence, and lastly $\nabla_{\perp}^2 \omega$ stands for the horizontal dissipation.

We can also write the temperature fluctuation equation:

$$\frac{\partial \theta'}{\partial t} + J(\Psi, \theta') + \omega \frac{\partial \bar{\theta}}{\partial Z} = \frac{1}{\sigma} \nabla_{\perp}^2 \theta \quad (12)$$

where $\partial \theta'/\partial t$ is the temperature fluctuation tendency, $J(\Psi, \theta')$ is the horizontal advection of temperature, $\omega \partial \bar{\theta}/\partial Z$ is the vertical advection of the mean temperature gradient (this is the only mean quantity which comes into this equation) and $1/\sigma \nabla_{\perp}^2 \theta$ is the horizontal diffusion of temperature fluctuation.

Finally, the mean temperature evolves on a slow time:

$$\frac{\partial \bar{\theta}}{\partial T} + \frac{\partial \overline{\theta' \omega'}}{\partial Z} = \frac{1}{\sigma} \frac{\partial^2 \bar{\theta}}{\partial Z^2} \quad (13)$$

where $\partial\bar{\theta}/\partial T$ represents the mean temperature tendency on the slow time, $\partial\overline{\theta'\omega'}/\partial Z$ is the large scale divergence of the eddy temperature flux and the overline denotes the horizontal average and average over fast time. Finally $1/\sigma \partial^2\bar{\theta}/\partial Z^2$ is the dissipation.

4 Numerical simulations

Numerical simulations [3, 4] have been performed with periodic boundary conditions using the Galerkin-Fourier approach in (x, y) direction and Chebyshev polynomials in the vertical direction z . The simulations have been done for a range of scaled Rayleigh numbers \tilde{Ra} and Prandtl numbers σ . The resolution has been varied with the scaled Rayleigh number \tilde{Ra} . A semi-implicit Runge-Kutta time stepping is used. The boundary conditions are impenetrable, fixed temperature, stress-free boundaries. Mathematically, it can be written as $\bar{\theta} = 1$ at $z = 0$, $\bar{\theta} = 0$ at $z = 1$, and $w = 0$, $\partial_z\Psi = 0$, $\theta' = 0$ at $z = 0$ and $z = 1$.

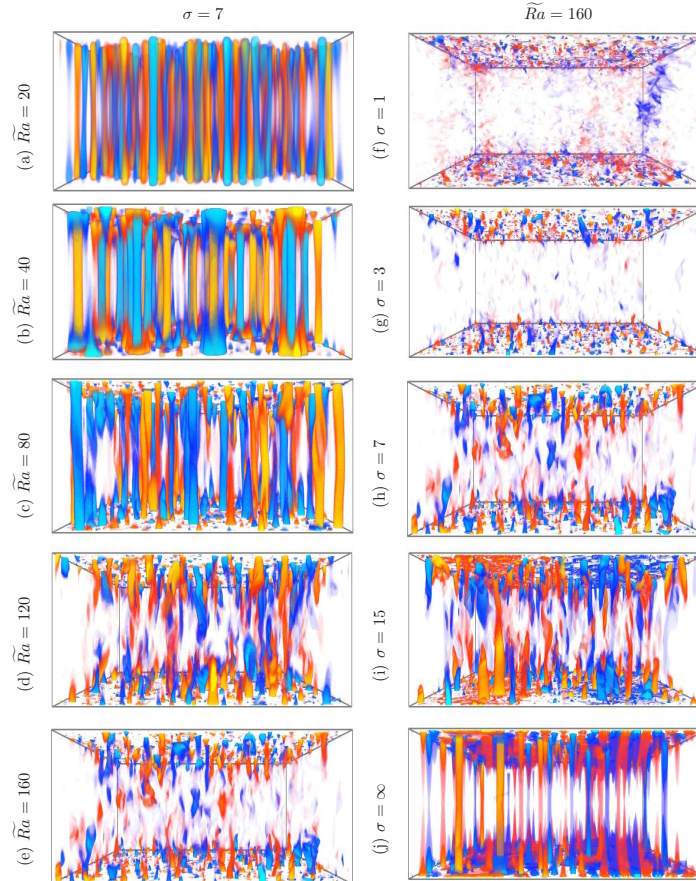


Figure 1. Volume renders of θ for $\sigma = 7$ and varying \tilde{Ra} (left) and $\tilde{Ra} = 160$ and varying σ (right).

Figure 2: Temperature fluctuations for various Rayleigh numbers and Prandtl numbers. From [4].

4.1 Observations

Figure 2 shows snapshot of the simulations for various Rayleigh and Prandtl numbers. The left column is for Prandtl number $\sigma = 7$ and the Rayleigh numbers increases from top to bottom. We see that we first have the presence of columns at low Rayleigh number, $\tilde{Ra} = 20$, here we are going to focus on this regime. Then, the Rayleigh number \tilde{Ra} increases and the columns start breaking up leading to a more turbulent regime. The right columns shows a fixed Rayleigh number, $\tilde{Ra} = 160$, with increasing Prandtl number going down. We see that increasing the Prandtl number leads to the appearance of columns. Note that there is no exact correspondence between varying the Prandtl and the Rayleigh number.

In summary, for rotating convection, columns are present for small Rayleigh number and/or large Prandtl number. In the following we are going to focus on this particular regime.

4.2 Convective Taylor Column regime

We consider the regime of convective Taylor columns. The simulation parameters are $\tilde{Ra} = E^{4/3} Ra = 40$, $\sigma = 7$ and the grid resolution in this case is $192 \times 192 \times 97$. Starting with arbitrary initial conditions, the temperature fluctuations relatively quickly organize into 2D convective columns. Hot plumes and cold plumes are present and the columns have nearly zero circulation. As a result they don't significantly advect each other in the horizontal direction. Moreover, the vorticity shows that fluid flows in opposite directions at the top and bottom with ring of vorticity around the center of the column. Also note that vorticity goes to zero at the mid-plane owing to symmetry.

4.3 Model of convective Taylor columns

To build a model of this convective Taylor columns, we seek steady nonlinear solution with axisymmetric structures [5]. It is also assumed that all the heat flux is carried by columns (this can be relaxed). Then we define c_f as the number of columns per units area and the Nusselt number by $Nu = -\partial_z \bar{\theta}(z = 0)$. Then, the set of equations for a single column become

$$\frac{\partial^2 \phi}{\partial Z^2} + \nabla_r^2 \left(\tilde{Ra} \frac{\partial \bar{\theta}}{\partial Z} + \nabla_r^4 \right) \phi = 0 \quad (14)$$

$$\frac{\partial \bar{\theta}}{\partial Z} + \frac{Nu}{1 + c_f \sigma \langle (\partial_r \phi)^2 \rangle} = 0 \quad (15)$$

where $\langle \rangle$ denotes the horizontal integral over column and ∇_r^2 is the radial component of the Laplacian.

4.4 Convective Taylor columns

The simplest solution of the set of equations (14)-(15) is a separable solution between the vertical and horizontal directions. First, consider horizontal Bessel function of first kind, $\phi(r, Z) = \hat{\phi}(Z) J_0(kr)$. The problem with this first solution is that there is an infinite heat flux and infinite circulation, we therefore need a cutoff. Moreover, another problem is that

this model fails to match numerical solution as the radial decay is too slow compared to the numerical simulations.

Therefore, we can improve the model by looking at Hankel functions, which are complex Bessel function defined by $H_0(kr) = J_0(kr) + iY_0(kr)$. Then the solution can be written as

$$\phi(r, Z) = \left(\frac{\pi}{8\sigma^2 c_f} \right)^{1/2} \phi(Z) H_0(kr) + c.c \quad (16)$$

where $c.c.$ denotes the complex conjugate. In this case the integral quantities (mass flux, heat flux, circulation) are finite, although there is a singularity at $r = 0$ which will be neglected because the integrated physical quantities are finite. If we take this ansatz in the equations (14)-(15), the vertical amplitude function $\phi(Z)$ is solution of an eigenvalue problem.

We can compare the analytical solutions to numerical simulations (see figure 3). We see that the solution based on Bessel functions (red curve) oscillates long after the actual structures goes to zero. The solution based on Hankel functions (blue curve) matches well with the numerical results for the radial solution. However for the axial profile, the Bessel functions gives a better results than Hankel functions. The horizontal oscillation is better captured by the Hankel solution than the Bessel functions.

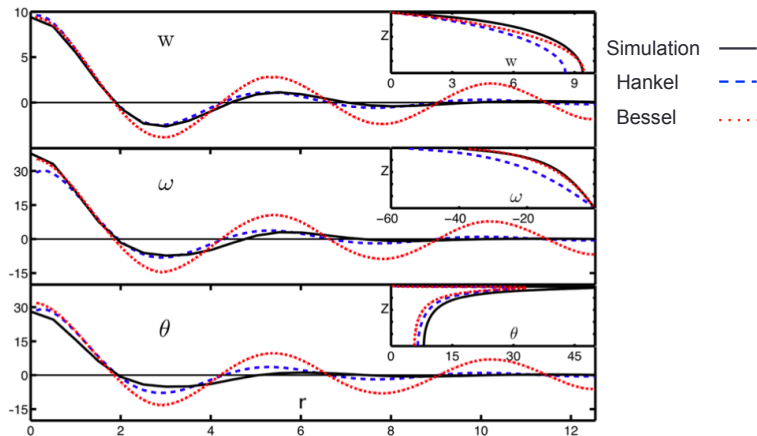


Figure 3: Radial and vertical (inset) profiles of the vertical velocity $w(z = 1/2, r)$, the vorticity $\omega(z = 1/96, r)$ and the temperature fluctuation $\theta(z = 1/96, r)$ solid line are the results of numerical simulations, blue dashed line is the solution based on Hankel function, and red dotted line the solution based on Bessel function. Note that the logarithmic singularity is present but nearly invisible. From [5].

5 Conclusion

We have seen that the non-hydrostatic quasi-geostrophic equations describe rapidly rotating convection. The numerical simulations show that there are several regimes of rotating

convection. Here, the focus is on the moderate forcing regime which has convective Taylor columns. The horizontal structure of these columns is well-described by an analytical model based on Hankel functions.

Ongoing work on the topic include the study of the turbulent regime and understanding the Lagrangian transport, which has implications for how tracers such as CO₂ are transported from surface to the deep ocean, and to construct a census to measure the population statistics of the columns.

References

- [1] Marshall, J. & Schott, F. 1999. Open-ocean convection: observations, theory and models. *Rev. Geophys.*, 37, 1-64.
- [2] Julien, K., Knobloch E., Milliff, R. and J. Werne, J. 2006. Generalized Quasi-Geostrophy for Spatially Anisotropic Rotationally Constrained Flows . *J. Fluid Mech.*, 555, 233-274.
- [3] Sprague, M., Julien, K., Knobloch, E. & Werne, J. 2006. Numerical Simulations of an Asymptotically Reduced System for Rotationally Constrained Convection. *J. Fluid Mech.*, 551, 141-174.
- [4] Julien, K., Rubio, A., Grooms, I. and Knobloch, E. Statistical and physical balances in low Rossby number Rayleigh-Benard convection. *Geophysical and Astrophysical Fluid Dynamics*, 2012, in press.
- [5] Grooms, I., Julien, K., Weiss, J.B. & Knobloch, E. 2010. A Model of Convective Taylor Columns in Rotating Rayleigh-Bénard Convection. *Phys. Rev. Lett.*, 104, 224501.